Which Parameters Determine the Type of Bogie Hunting Bifurcation?

Oldrich Polach[1] and Jonas Vuitton[2]

[1] Independent consultant and assessor, Neuhausen am Rheinfall, Switzerland
o@polach.ch
[2] Technische Universität Berlin, Chair of Rail Vehicles, Germany

Abstract. An important question of railway vehicle dynamics is to understand which parameters affect the transformation between sub- and supercritical bifurcation in the stability assessment. Recent studies report effects of the equivalent conicity, the wheelset guidance stiffness and other parameters. Performing parameter variations using a typical bogie model with linear suspension components but considering all nonlinearities of wheel/rail contact geometry, this paper shows that the type of bifurcation depends predominantly on the nonlinearity of the wheel/rail contact geometry, while the effects of the equivalent conicity, the creep forces and the wheelset guidance stiffness are less important.

Keywords: Bogie Hunting, Bifurcation, Stability, Equivalent Conicity.

1 Introduction

Bogie hunting is an important safety phenomenon in context of railway vehicle dynamics. A bifurcation diagram displaying the amplitude of the lateral wheelset oscillation as a function of speed is used to show the multiplicity of solutions in nonlinear railway vehicle dynamics. Fig. 1a shows an example of subcritical Hopf bifurcation: The branching solution drawn in dashed line arising at the Hopf bifurcation point (corresponding to the linear critical speed v_{lin}) is unstable and coexists with the stationary solution. Fig. 1b displays an example of supercritical Hopf bifurcation where the new branch is stable.

Investigation of Hopf bifurcation of railway vehicles and its subsystems is topic of various research studies. From the point of view of railway practice, the main interest concerns the nonlinear critical speed v_{nlin}, which is defined either by the saddle-node bifurcation (Fig. 1a) or by the Hopf bifurcation (Fig. 1b). In Fig. 1a displaying subcritical Hopf bifurcation, the range of speeds $\Delta v = v_{\mathrm{lin}} - v_{\mathrm{nlin}}$ represents an "uncertain region" [1] in which the dynamic performance of the railway vehicle largely depends on the initial conditions. A wheelset oscillation with a large amplitude from flange to flange can start at any speed inside the uncertain region Δv. In case of a supercritical bifurcation diagram as shown in Fig. 1b, there is no uncertain region ($\Delta v = 0$). A wheelset oscillation with a very small amplitude starts at speed $v_{\mathrm{lin}} = v_{\mathrm{nlin}}$ and increases steadily with growing vehicle speed.

The bifurcation diagram of railway vehicles can take various shapes, affected by many parameters, and especially by system nonlinearities, as shown in Fig. 1c and 1d. Multiple solutions can be present outside of the uncertain region Δv as well as if $\Delta v = 0$. However, only the uncertain region Δv is of major importance for railway practice as there can be either a wheelset oscillation with a large amplitude or a smooth run for the same speed. Therefore, all possible shapes of bifurcation diagrams can be assigned to either one of the two generic types of bifurcation diagrams shown in Fig. 1a and 1b. In this paper, these two basic categories are called subcritical ($\Delta v > 0$) or supercritical ($\Delta v = 0$) bifurcation diagram, respectively. The terms subcritical and supercritical as used in this paper refer thus to the presence of an uncertain region of speed Δv and not to the Hopf bifurcation itself.

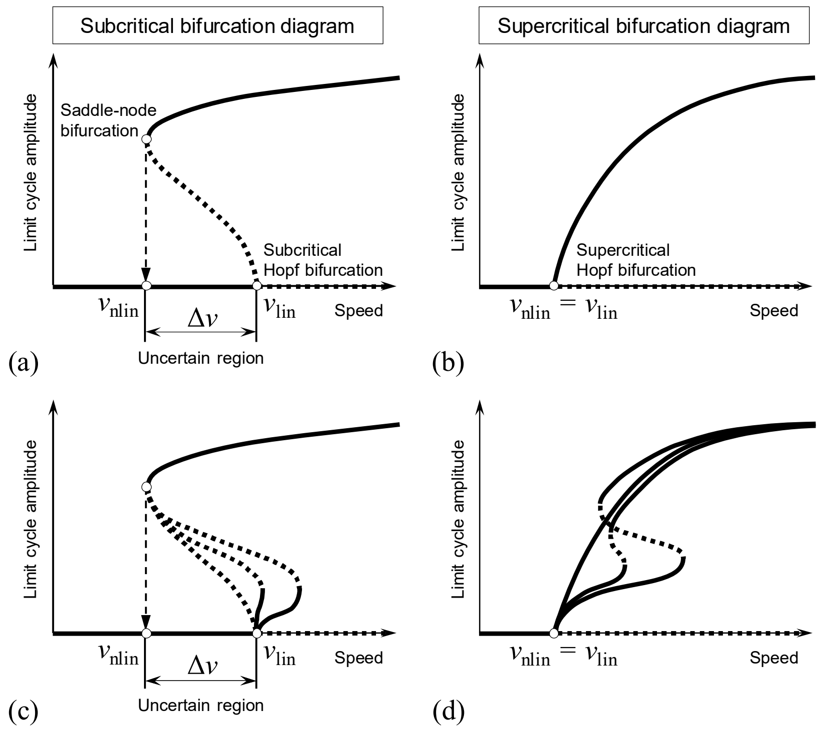

Fig. 1. Two basic types of bifurcation diagrams as classified in this paper (top diagrams) and possible variants related to them (bottom diagrams).

These two basic types of bifurcation diagrams differ significantly in terms of the behaviour of the vehicles at the stability limit. The knowledge of the bifurcation diagram for a particular vehicle and running conditions allows a better understanding of test results. In case of a subcritical bifurcation diagram, the self-excited hunting movement can occur suddenly. It is therefore not possible to estimate the margin before reaching the critical speed and exceeding the safety limits. Even a very smooth run at a given speed does not guarantee a great margin for speed increase before reaching the safety limits. In case of a supercritical bifurcation diagram, on the other hand, the amplitude of the wheelset oscillations increases slowly with increasing speed, and a limit cycle with small wheelset amplitude is often present without exceedance of safety limits. The question of which parameters influence the type of bifurcation diagrams is therefore of great importance in the railway practice.

Several publications investigated the bifurcation diagram of railway vehicles. Polach [2, 3] showed the effect of the nonlinearity in the wheel/rail contact geometry on the type of bifurcation diagrams. Recent publications [1, 4, 5] provided results regarding the impact of the equivalent conicity and the wheelset guidance stiffness on the type of Hopf bifurcation. An investigation of a suspended wheelset model in [1] reports that the longitudinal stiffness of the primary suspension (i.e. the wheelset guidance) has a great influence on the bifurcation diagram, changing from subcritical to supercritical with increasing stiffness. A theoretical and numerical investigation of a railway bogie in [4] presents similar conclusions regarding the influence of the longitudinal stiffness of the primary suspension. A parameter study of two China's high-speed vehicle types in [5] concludes that the primary lateral wheelset guidance stiffness and the creep coefficient have a great influence on the type of bifurcation.

However, previous publications did not adequately identify how the type of bifurcation is affected by the nonlinearities of the wheel/rail contact, and which parameters determine the type of bifurcation for vehicles with linear suspension parameters. This paper investigates the parameters influencing the type of bogie hunting bifurcation diagram using a model with linear suspension and wheelset guidance parameters while considering all nonlinearities of the wheel/rail contact.

2 Simulation Model and Parameters

The investigation was carried out using a three-dimensional nonlinear half-vehicle model with one 2-axle bogie in multi-body simulation tool SIMPACK [6]. The movements of the car body have been restricted to its vertical translation and it has been ensured that the simplified model has a similar dynamic behaviour as a model of the complete vehicle.

The model of wheel/rail contact is described by the contact geometry, as well as with a creep force model. The equivalent conicity λ_{eq} is used in railway practice to characterise the wheel/rail contact geometry in regard to running dynamics and stability. Previous research of the first author [2, 3] identified an important effect of the nonlinearity of wheel/rail contact geometry on the bifurcation behaviour of railway vehicles. A new, additional parameter called nonlinearity parameter N_P has been introduced to characterise this effect in [3, 7]. It is defined as the slope of the conicity function between the conicity value λ_2 for the wheelset displacement amplitude of 2 mm and the conicity value λ_4 for the wheelset displacement amplitude of 4 mm:

$$N_P = \frac{\lambda_4 - \lambda_2}{2} \quad [\mathrm{mm}^{-1}] \tag{1}$$

To investigate thoroughly the effect of wheel/rail contact geometry, a set of 12 wheel and rail profile combinations was developed with equivalent conicities λ_{eq} of 0.1, 0.2, 0.3 and 0.4 for an amplitude of 3 mm, and with three differing values of N_P for each value of λ_{eq}. It is hardly possible to design profile combinations with a given value of λ_{eq} together with a target value of N_P. Therefore, the target for N_P distinguishes only between zero, and positive and negative value. The target contact geometries were achieved by modifying the wheel and rail profiles and rail inclination as well as by a slight variation of the track gauge around the nominal value of 1435 mm. The equivalent conicity functions of the applied contact geometries can be seen in Fig. 2.

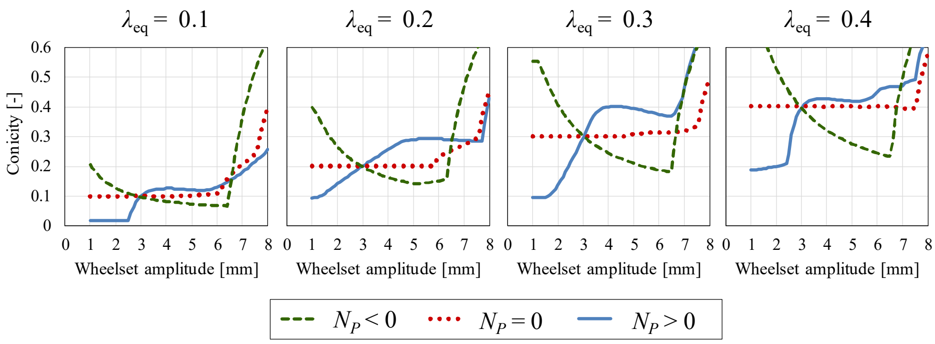

Fig. 2. Equivalent conicity functions of wheel/rail contact geometries used in this study.

The wheel/rail creep forces are computed using FASTSIM implemented in SIMPACK. The input parameters characterising the conditions between wheel and rail are the friction coefficient μ and the Kalker-factor k_K, a weighting parameter reducing the initial slope of the creep force curve.

The basic variant of the simulation model has the following parameters:

- wheel/rail creep force model (dry rail): $\mu = 0.4$, $k_K = 1$
- wheelset guidance stiffness per wheel: $k_{1x} = 8$ kN/mm, $k_{1y} = 8$ kN/mm.

The investigations of hunting bifurcation were carried out varying the following parameters of the nonlinear wheel/rail contact model:

- equivalent conicity λ_{eq}: 0.1, 0.2, 0.3 and 0.4
- nonlinearity parameter: $N_P > 0$, $N_P = 0$ and $N_P < 0$
- wheel/rail friction coefficient μ: 0.1, 0.2, 0.3, 0.4, 0.5 and 0.6
- Kalker-factor k_K: 0.25, 0.50, 0.75 and 1.

Regarding the vehicle parameters, the longitudinal k_{1x} and lateral k_{1y} wheelset guidance stiffness are known to have an important effect on the bogie stability. Both stiffness values k_{1x} and k_{1y} were varied between 2 kN/mm and 64 kN/mm.

3 Procedure Applied for Investigations

The computation of the nonlinear critical speed v_{nlin} was carried out by "ramping": Starting from an unstable speed, the vehicle runs in limit cycle on an ideal track, reducing the speed very slowly. The nonlinear critical speed is reached when the hunting motion disappears.

The linear critical speed v_{lin} was evaluated by a set of simulations at constant speed, applying a very small disturbance of 0.2 mm in the lateral direction. At any given speed, a damping out of the hunting motion means a stable behaviour, and the presence of sustaining oscillations means an instable behaviour. If the linear and nonlinear critical speeds are the same ($\Delta v \rightarrow 0$), the bifurcation diagram is of the supercritical type, otherwise it is subcritical with an uncertain region $\Delta v = v_{\mathrm{lin}} - v_{\mathrm{nlin}}$.

4 Results

Fig. 3 shows exemplarily the effect of the longitudinal wheelset guidance stiffness k_{1x} on the nonlinear critical speed v_{nlin} and on the uncertain region Δv for the lateral wheelset guidance stiffness $k_{1y} = 2$ kN/mm. The nonlinear critical speed increases with growing stiffness and reaches saturation at wheelset guidance stiffness values of about 20 kN/mm, which corresponds to typical properties of railway vehicles. The supercritical bifurcation ($\Delta v = 0$) occurs for wheel/rail contact geometry with $N_P < 0$, and for $N_P = 0$ (conical profiles) for high values of longitudinal wheelset guidance stiffness and high equivalent conicity values, while there is a subcritical bifurcation for other parameter combinations.

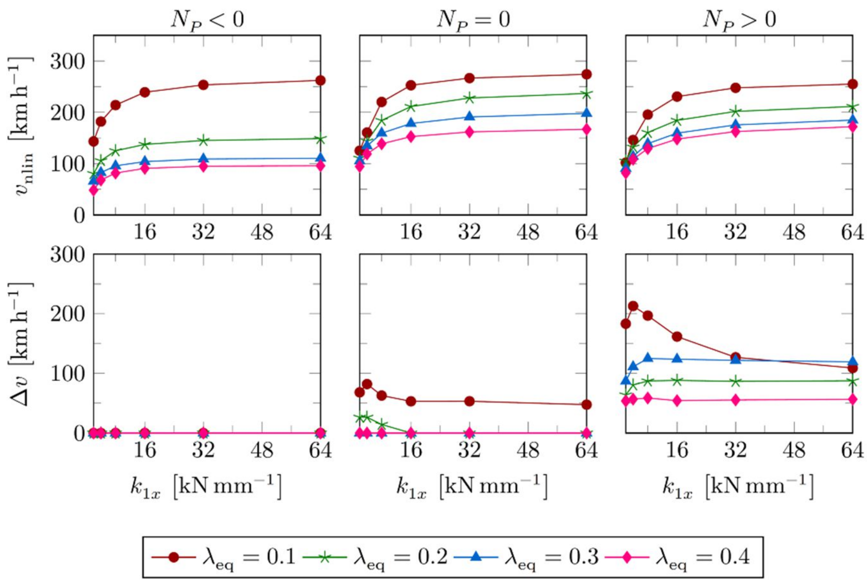

Fig. 3. Nonlinear critical speed and the uncertain region Δv in function of longitudinal wheelset guidance stiffness for different wheel/rail contact geometries.

In the following we investigate the difference between the subcritical and supercritical bifurcation diagram in dependency on parameter variation of the wheel/rail creep force model and the wheelset guidance stiffness. Fig. 4 shows the switch between the subcritical and supercritical bifurcation, evaluated for the basic wheelset guidance stiffness parameters $k_{1x} = 8$ kN/mm and $k_{1y} = 8$ kN/mm, in dependency on creep force parameters friction coefficient μ and Kalker-factor k_K. A supercritical bifurcation (uncertain region speed range $\Delta v = 0$) is represented by white colour, the subcritical bifurcation with $\Delta v > 20$ km/h by dark colour. The subcritical bifurcation with a small uncertain region Δv between 0 km/h and 20 km/h is displayed in light colour to differentiate between a very pronounced and a less distinctive subcritical form of the bifurcation diagram. For $N_P < 0$, a supercritical bifurcation ($\Delta v = 0$) is present for all creep force parameters with exception of combination $\mu = 0.1$ and $k_K = 1$, at which there is a subcritical diagram with a small Δv. For $N_P > 0$, there is a subcritical bifurcation for almost all cases with $k_K = 0.5$, 0.75 and 1. Considering coned wheel profiles, both the subcritical and the supercritical type of bifurcation are present. The nonlinearity parameter clearly shows the biggest influence on the type of bifurcation diagram, followed by the Kalker-factor, while the wheel/rail friction coefficient and the equivalent conicity have a rather little influence.

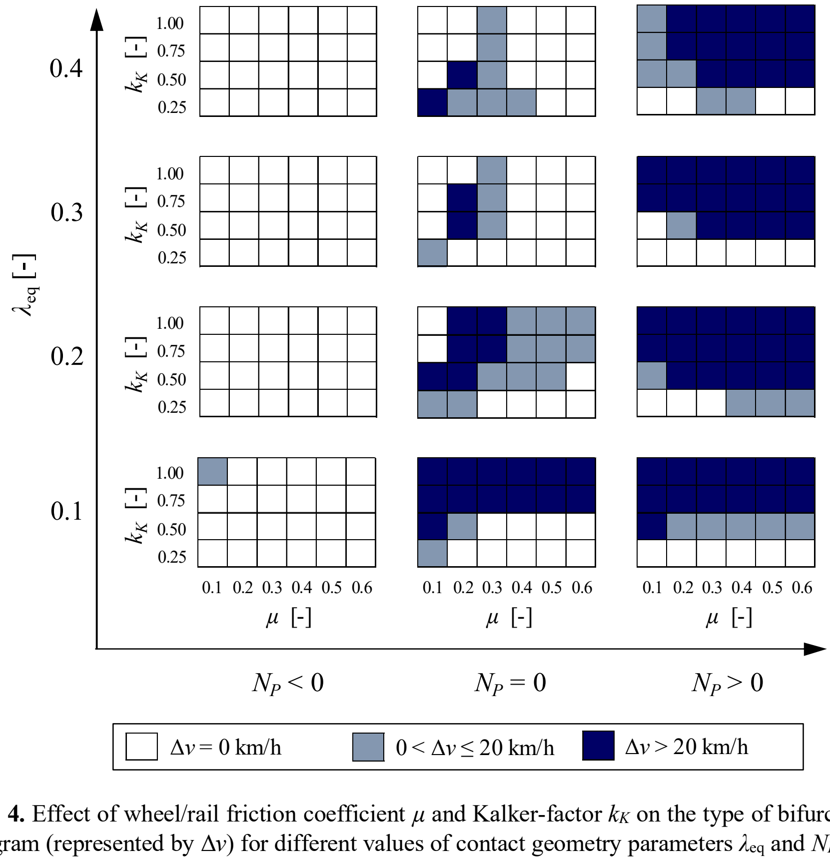

Fig. 4. Effect of wheel/rail friction coefficient μ and Kalker-factor k_K on the type of bifurcation diagram (represented by Δv) for different values of contact geometry parameters λ_{eq} and N_P.

Fig. 5 shows the change between subcritical and supercritical bifurcation in dependency of wheelset guidance stiffness k_{1x} and k_{1y} using the base wheel/rail creep force parameters $\mu = 0.4$ and $k_K = 1$. In contrast to the other diagrams, the scaling of stiffness axes is not linear in regard to provide better resolution for the low stiffness at which the critical speed is more affected (see Fig. 3). Similarly, as for the variation of the creep force parameters, the nonlinearity parameter N_P has the biggest influence on the type of bifurcation while the effect of the equivalent conicity λ_{eq} is very small. The impact of the wheelset guidance stiffness is most important for coned wheels ($N_P = 0$).

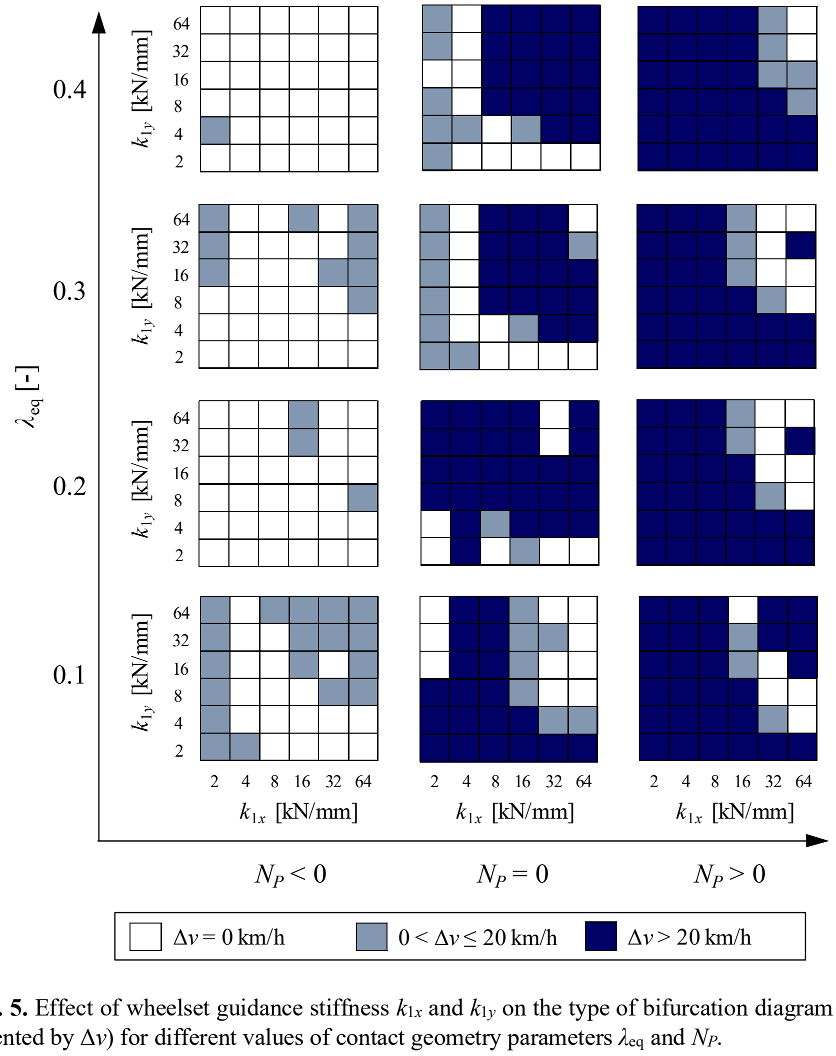

Fig. 5. Effect of wheelset guidance stiffness k_{1x} and k_{1y} on the type of bifurcation diagram (represented by Δv) for different values of contact geometry parameters λ_{eq} and N_P.

5 Conclusions

The investigations using nonlinear time step simulation demonstrate that for a model with linear suspension and wheelset guidance parameters, the nonlinearity parameter N_P predominantly influences the transformation between the subcritical and the supercritical type of bifurcation diagram. A subcritical bifurcation mostly occurs for $N_P > 0$, and a supercritical bifurcation for $N_P < 0$, confirming the results obtained with full nonlinear vehicle models [3]. However, there are some deviations from this rule, particularly for small Kalker-factor and for low equivalent conicity. The wheelset guidance stiffness also has an effect on the bifurcation, particularly for coned wheel profiles ($N_P = 0$), which, however, do not correspond to the actual wheel profiles in railway practice.

Comparing our results with publications [1, 4, 5], some similarities can be observed. However, our investigation clearly shows the biggest influence of the nonlinearity of the wheel/rail contact geometry. This effect was not considered in [1, 4, 5], as coned wheels with a simplified flange contact described by a force function were used. The presented results demonstrate that the investigations using simplifications in the modelling of nonlinear wheel/rail contact geometry cannot be considered as trustworthy because they neglect the dominating effect of the contact nonlinearity.

References

1. Wu, X., Chi, M.: Parameters study of Hopf bifurcation in railway vehicle system. Journal of Computational and Nonlinear Dynamics 10(3), (2015).
2. Polach, O.: On non-linear methods of bogie stability assessment using computer simulations. Proc IMechE Part F: J Rail and Rapid Transit 220(1), 13-27 (2006).
3. Polach, O.: Characteristic parameters of nonlinear wheel/rail contact geometry. Vehicle System Dynamics, 48(S1), 19-36 (2010).
4. Zhang, T., True, H., Dai, H.: A codimension two bifurcation in a railway bogie system. Arch Appl Mech 88(3), 391–404 (2018).
5. Dong, H., Zeng, J., Xie, J., Jia, L.: Bifurcation\instability forms of high speed railway vehicles. Science China, Technological Sciences 56(7), 1685–1696 (2013).
6. Vuitton, J.: Nichtlineare Fahrwerkdynamik an der Stabilitätsgrenze. Master thesis, Technische Universität, Berlin (2018).
7. Polach, O., Nicklisch, D.: Wheel/rail contact geometry parameters in regard to vehicle behaviour and their alteration with wear. Wear 366-367, 200-208 (2016).